



A complete glacier inventory of the Antarctic Peninsula based on Landsat 7 images from 2000 to 2002 and other preexisting data sets

Jacqueline Huber¹, Alison J. Cook^{2,3}, Frank Paul¹, and Michael Zemp¹

¹Department of Geography, University of Zürich–Irchel, Zürich, 8057, Switzerland

²Department of Geography, Swansea University, Swansea, SA2 8PP, UK

³Department of Geography, Durham University, Durham, DH1 3LE, UK

Correspondence to: Jacqueline Huber (jhuber@access.uzh.ch)

Received: 7 September 2016 – Discussion started: 15 September 2016

Revised: 3 January 2017 – Accepted: 11 January 2017 – Published: 15 February 2017

Abstract. The glaciers on the Antarctic Peninsula (AP) potentially make a large contribution to sea level rise. However, this contribution has been difficult to estimate since no complete glacier inventory (outlines, attributes, separation from the ice sheet) is available. This work fills the gap and presents a new glacier inventory of the AP north of 70° S, based on digitally combining preexisting data sets with geographic information system (GIS) techniques. Rock outcrops have been removed from the glacier basin outlines of Cook et al. (2014) by intersection with the latest layer of the Antarctic Digital Database (Burton-Johnson et al., 2016). Glacier-specific topographic parameters (e.g., mean elevation, slope and aspect) as well as hypsometry have been calculated from the DEM of Cook et al. (2012). We also assigned connectivity levels to all glaciers following the concept by Rastner et al. (2012). Moreover, the bedrock data set of Huss and Farinotti (2014) enabled us to add ice thickness and volume for each glacier.

The new inventory is available from the Global Land Ice Measurements from Space (GLIMS) database (doi:10.7265/N5V98602) and consists of 1589 glaciers covering an area of 95 273 km², slightly more than the 89 720 km² covered by glaciers surrounding the Greenland Ice Sheet. Hence, compared to the preexisting data set of Cook et al. (2014), this data set covers a smaller area and one glacier less due to the intersection with the rock outcrop data set. The total estimated ice volume is 34 590 km³, of which one-third is below sea level. The hypsometric curve has a bimodal shape due to the unique topography of the AP, which consists mainly of ice caps with outlet glaciers. Most of the glacierized area is located at 200–500 m a.s.l., with a secondary maximum at 1500–1900 m. Approximately 63 % of the area is drained by marine-terminating glaciers, and ice-shelf tributary glaciers cover 35 % of the area. This combination indicates a high sensitivity of the glaciers to climate change for several reasons: (1) only slightly rising equilibrium-line altitudes would expose huge additional areas to ablation, (2) rising ocean temperatures increase melting of marine terminating glaciers, and (3) ice shelves have a buttressing effect on their feeding glaciers and their collapse would alter glacier dynamics and strongly enhance ice loss (Rott et al., 2011). The new inventory should facilitate modeling of the related effects using approaches tailored to glaciers for a more accurate determination of their future evolution and contribution to sea level rise.

1 Introduction

The ice masses of the Antarctic Peninsula (AP) potentially make a large contribution to sea level rise (SLR) since a large amount of water is stored in the ice and a high sensitivity to temperature increase has been reported (Hock et al., 2009). However, the glaciers on the AP were not separately taken into account for their individual sea level contribution in the Fifth Assessment Report of the IPCC (Vaughan et al., 2013) because a complete glacier inventory of the AP was not available at that time. As a result, only the ice masses of the surrounding islands were considered from the inventory compiled by Bliss et al. (2013). The freely available data sets for the AP were incomplete and of a varied nature (see Fig. 1), ranging from the World Glacier Inventory (WGI; WGMS and NSIDC, 2012), which provides extended parameters for most of the glaciers on the AP from the second half of the 20th century but without area information and only available as point data, to the vector data sets (two-dimensional outlines) from the Global Land Ice Measurements from Space (GLIMS; GLIMS and NSIDC, 2015) database and the Randolph Glacier Inventory (RGI; Arendt et al., 2015), which were spatially incomplete. Moreover, the spatial overlap of the WGI with the boundaries of individual glaciers in the RGI was limited (Fig. 1) so that an automated digital intersection (spatial join) for parameter transfer was not possible.

Conversely, for Graham Land, representing the part of the AP north of 70° S, several more specific data sets exist that could be combined for a full and coherent glacier inventory: a detailed 100 m resolution DEM was prepared by Cook et al. (2012); glacier catchment outlines based on this DEM and the Landsat Image Mosaic of Antarctica (LIMA; Bind-schadler et al., 2008) were derived by Cook et al. (2014); a recently updated data set of rock outcrops for all of Antarctica is available from the Antarctic Digital Database (ADD; <http://www.add.scar.org/home/add7>); a modeled raster data set of bedrock topography is available from Huss and Farinotti (2014).

Here, we present the first comprehensive glacier inventory of the Antarctic Peninsula north of 70° S (Graham Land) and describe methods used to digitally combine the existing data sets. The final outline data set of the AP is supplemented with several glacier-specific parameters, such as topographic information and hypsometry, and thickness and volume information, as well as the earlier classification of glacier front characteristics. With these parameters we analyze similarities and differences with other glacierized regions, as well as glacier-specific contributions to sea level and climate sensitivities. For a clear handling by different modeling and remote sensing communities, each glacier is assigned one of three connectivity levels to the ice sheet (CL0 is no connection, CL1 is a weak connection and CL2 is a strong connection) following the approach introduced by Rastner et al. (2012) to separate the peripheral glaciers on Greenland from the ice sheet.

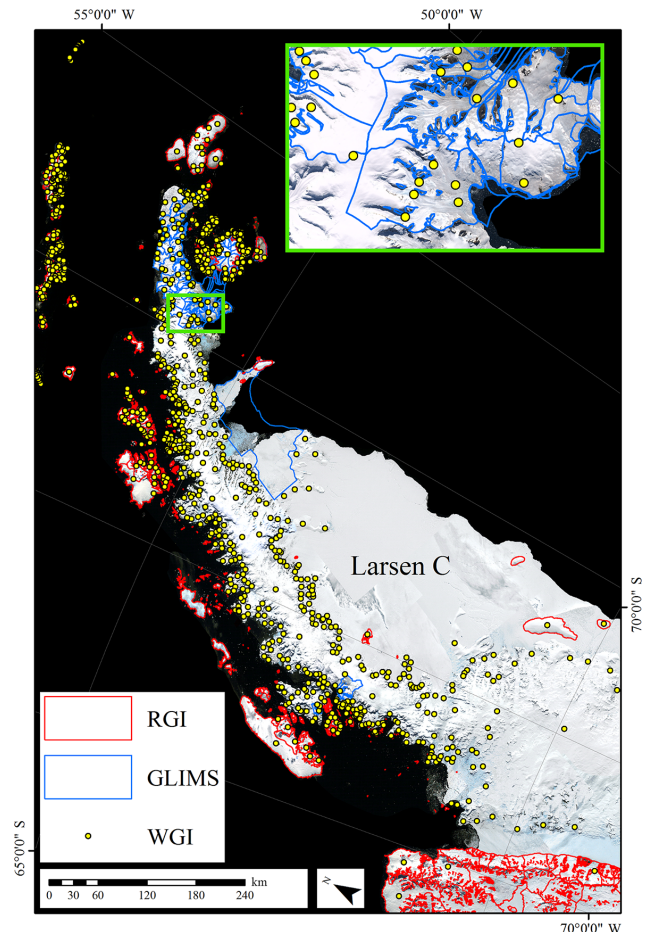


Figure 1. Landsat Image Mosaic of Antarctica (LIMA) overlaid by existing GLIMS and RGI glacier outlines and WGI glacier point locations for Graham Land on the AP. Inset map illustrating that the distribution of the WGI points does not enable assignment of points to individual glacier outlines.

2 Study region

The AP extends northwards of the mainland from approximately 75° S for more than 1500 km northeasterly to 63° S, and it is enclosed to the west by the Bellingshausen Sea and to the east by the Weddell Sea of the Southern Ocean. The part of the AP north of 70° S represents Graham Land and its peripheral islands, for which the glacier inventory is created. The South Shetland Islands are not regarded as being part of the AP and are therefore not included in the present inventory. The central part of the mainland is dominated by a narrow mountain chain with a mean height of 1500 m (maximum 3172 m) and an average width of 70 km. The unique topography, with an interior high-elevation plateau surrounded by steep slopes and flat valley bottoms results in distinct glacier types. In general, the highest regions are covered by ice caps, and much lower-lying valley glaciers are either connected to them and heavily crevassed in the steep regions,

or they are entirely separated from them, uncovering several rock outcrops.

The AP has a polar-to-subpolar maritime climate, but the climatic and oceanographic regime varies across the AP, causing varying glacier dynamics (Arigony-Neto et al., 2014). The often polythermal glaciers experience a distinct melting period in austral summer, particularly the glaciers in the northern part of the AP. The special topographic characteristics of the AP make the flat, low-lying parts of its glaciers particularly vulnerable to climate change: for example, a small increase in temperature might cause large parts of their area to become ablation regions; most of them are marine-terminating glaciers that also experience melt from surrounding ocean waters (Cook et al., 2016), and many of them nourish ice shelves (Cook et al., 2014) that currently buttress them but can quickly disappear (Rott et al., 1996) causing rapid shrinkage of the related glaciers (Rott et al., 1996; Hulbe et al., 2008).

Since the early 1950s, significant atmospheric warming trends (Turner et al., 2009) and increasing ocean temperatures (Shepherd et al., 2003) have been observed across the AP. As a consequence, ice shelves are collapsing and glacier fronts are retreating (Pritchard and Vaughan, 2007; Davies et al., 2012; Cook et al., 2014, 2016). Conversely, knowledge about the mass balance of the glaciers of the AP is sparse (Rignot and Thomas, 2002), although a few studies exist that indicate a general mass loss (Helm et al., 2014; Kunz et al., 2012).

For the purpose of this study, the AP is additionally divided into four sectors (NW, NE, SW and SE) to reveal differences between climatically different regions of the AP. The division west–east is based on the main topographic divide, and north–south is based on the 66° S latitude.

3 Data sets

This section gives a short description of the preexisting data sets covering the AP (Graham Land) that are used for generating the glacier inventory. Table 1 summarizes their key characteristics, presenting their content, sources, access, references and application in this study. The following data sets are used:

1. the digital elevation model (DEM) by Cook et al. (2012);
2. the glacier catchment outlines by Cook et al. (2014);
3. the rock outcrop data set of Antarctica by Burton-Johnson et al. (2016);
4. the bedrock elevation grid by Huss and Farinotti (2014);
5. the Antarctic ice-sheet drainage divides by Zwally et al. (2012) and

6. the Landsat Image Mosaic of Antarctica (LIMA) by Bindschadler et al. (2008).

3.1 Digital elevation model

Cook et al. (2012) generated a 100 m resolution DEM of the AP (63–70° S), which is available from the National Snow and Ice Data Center (NSIDC; <http://nsidc.org/data/NSIDC-0516>) in the WGS84 Stereographic South Pole projection. This DEM is an improvement of the ASTER Global Digital Elevation Model (GDEM) product, which locally contained large errors and artifacts (see Cook et al., 2012). The accuracy of the DEM is in particular improved on gentle slopes of the high plateau region. However, they removed small anomalies, which has resulted in small inherent gaps along the coast, and some islands are missing (Cook et al., 2012). As a result, the DEM does not entirely cover the study region (approximately 1 % of the area is missing). This DEM has also been used by Cook et al. (2014) for the generation of catchment outlines (see next section) and is used in this study for the calculation of glacier-specific parameters (see Sect. 4.3) for the glacierized areas it covers.

3.2 Catchment outlines

Glacier inventories, such as those available in GLIMS or the RGI, require glaciers to be separated into individual entities (Paul et al., 2009). This can be accomplished by intersecting drainage divides derived from watershed analysis (e.g., Bolch et al., 2010; Kienholz et al., 2013) with outlines of glacier extents derived from semiautomated mapping techniques (e.g., Paul et al., 2002). Cook et al. (2014) automatically delineated glacier catchments of the AP in ArcGIS from ESRI by applying hydrological tools to the DEM described above (Fig. 2). They digitized the AP coastline and some islands in that data set based on images acquired by Landsat 7 between 2000 and 2002 for the LIMA (Bindschadler et al., 2008). Since the DEM misses some islands around the AP, mainly in the central western region, the drainage divide analysis is missing for these regions. Additionally, they used grounding lines from the Antarctic Surface Accumulation and Ice Discharge (ASAIID) project data source (Bindschadler et al., 2011), modified in places with features visible on the LIMA to divide glaciers from ice shelves. Furthermore, the ice-velocity data set of Rignot et al. (2011) was considered by Cook et al. (2014) to manually verify and adjust the lateral boundaries of glaciers.

The resulting data set consists of 1590 glacier catchment outlines for the AP with an area of 96 982 km², covering the region between 63 and 70° S. Islands smaller than 0.5 km² and ice shelves are excluded. The data set provides a consistent time period of all basins and includes several parameters for each basin, such as location, time stamp, area, and a classification of glacier type, form and front. The definition of the parameters and category numbers conform to the

Table 1. Data sets used for the generation of the glacier inventory and a description of their properties.

	DEM	Glacier catchment outlines	Rock outcrops	Bedrock elevation grid	Antarctic ice-sheet drainage divides
Content	Elevation on a 100 m grid of the AP (Graham Land, 63–70° S)	Inventory of 1590 glacier basins of the AP (Graham Land, 63–70° S) on the mainland and surrounding islands	New rock outcrop data set for Antarctica	Bedrock data set for the AP (Graham Land, 63–70° S) on a 100 m grid	Drainage divides of the Antarctic ice sheet
Sources	ASTER Global Digital Elevation Model (GDEM)	DEM of Cook et al. (2012), LIMA (Bindshadler et al., 2008), grounding line based on the Antarctic Surface Accumulation and Ice Discharge (ASAIID) project data source (Bindshadler et al., 2011)	Landsat 8 data	Simple ice-dynamic modeling with a variety of available data sets (surface mass balance, point ice thickness and ice flow velocity)	GLAS/CESat 500 m laser altimetry DEM (DiMarzio, 2007) Landsat Image Mosaic of Antarctica (LIMA; Bindshadler et al., 2008) and the MODIS Mosaic of Antarctica (Haran et al., 2005)
Access	http://nsidc.org/data/	http://add.scar.org/ (available only with a limited number of attributes)	http://add.scar.org/	Available online from the article's supplement (doi:10.5194/tc-8-1261-2014-supplement)	http://icesat4.gsfc.nasa.gov/cryo
Reference	Cook et al. (2012)	Cook et al. (2014)	Burton-Johnson et al. (2016)	Huss and Farinotti (2014)	Zwally et al. (2012)
Application in this study	Calculation of (a) glacier-specific topographic parameters (min, max, mean, median elevation, slope, aspect), (b) overall and glacier specific hypsometry, and (c) thickness grid combined with the bedrock elevation grid of Huss and Farinotti (2014)	Initial data set for the generation of glacier outlines	Used to remove the (ice-free) rock outcrops from the glacier catchment outlines to generate glacier outlines	Calculation of the thickness grid combined with the DEM of Cook et al. (2012)	Separation of the glaciers from the ice sheet

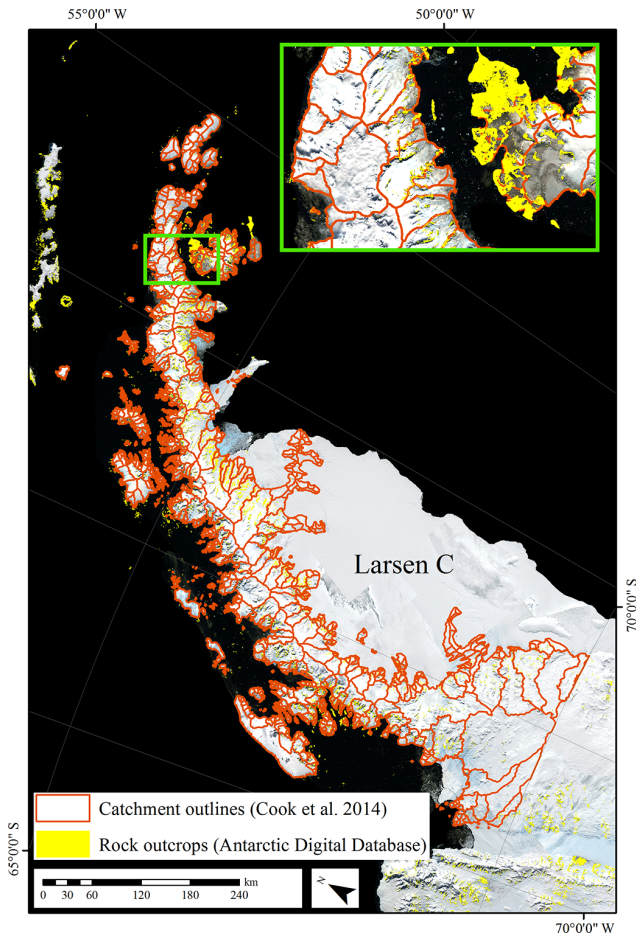


Figure 2. Glacier catchment outlines of Cook et al. (2014) and the newest rock outcrop data set from Burton-Johnson et al. (2016) overlaying the LIMA.

GLIMS classification system provided by the GLIMS Classification Manual (Rau et al., 2005) and based on the UNESCO (1970) guidelines as well as the Glossary of Glacier Mass Balance (Cogley et al., 2011). However, topographic parameters such as minimum, maximum, mean, and median elevation, or mean slope and aspect, are missing.

This catchment outline data set is available from the Scientific Committee on Antarctic Research (SCAR) ADD (<http://add.scar.org/home/add7>; ADD Consortium, 2012), but it does not include any of the glacier-specific attributes mentioned above aside from area and length. The data set with the complete information has not been published so far and has been generated and provided by A. Cook in the framework of this study in the WGS84 Stereographic South Pole projection. Whereas the catchment outlines provide a solid foundation for the generation of a glacier inventory, rock outcrops are part of the glacierized area and need to be removed (Raup and Khalsa, 2010).

3.3 Rock outcrops

The ADD website (www.add.scar.org) provides a detailed vector data set of rock outcrop boundaries in the WGS84 Stereographic South Pole projection that has recently been updated (see Burton-Johnson et al., 2016). A former rock outcrop data set, which has already been used (by Bliss et al. (2013) for instance) to create the inventory for the glaciers of the islands surrounding Antarctica, originated from a digitization of outcrops from different maps prepared in the 1990s at different scales and with variable accuracy. As a result, the data set has some major georeferencing inconsistencies, misclassifications and overestimations of the ice-free area of Antarctica (Burton-Johnson et al., 2016). The recently improved data set of exposed rock outcrops by Burton-Johnson et al. (2016) used here (Fig. 2), overcomes these issues and has a much better accuracy. It is based on a new automated method that identifies sunlit as well as shaded rock outcrops using multispectral classification of Landsat 8 satellite imagery. They manually removed incorrectly classified pixels (illuminated and shaded) such as snow, clouds and liquid water. The new data set reveals that 0.18 % of the total area of Antarctica is rock outcrops, which is approximately one-half of previous estimates (Burton-Johnson et al., 2016).

3.4 Bedrock elevation grid

Huss and Farinotti (2014) derived a new bedrock elevation grid with 100 m spatial resolution as well as the related ice thickness grid based on glacier surface topography and simple ice-dynamic modeling. Compared to the Bedmap2 data set by Fretwell et al. (2013) with a resolution of 1 km, the new version also captures the rugged subglacial topography in great detail. The narrow and deep subglacial valleys that are often below sea level are more accurately represented, allowing the modeling of even small-scale processes.

Their data set is available online from the article supplement (doi:10.5194/tc-8-1261-2014-supplement) on WGS84 Antarctic Polar Stereographic projection. Their data set already excluded the rock outcrops using the former version of the ADD (ADD Consortium, 2012). Since we have used the updated version of the rock outcrops data set for creating the glacier inventory, a new thickness grid is calculated (see Sect. 4.1).

3.5 Antarctic ice-sheet drainage divides

The Cryosphere Science Laboratory of NASA's Earth Sciences Divisions (Zwally et al., 2012) provides an Antarctic ice-sheet drainage divide data set developed by the Goddard Ice Altimetry Group from ICESat data based on the GLAS/ICESat 500 m laser altimetry DEM (DiMarzio, 2007). They used other sources, such as LIMA (Bindschadler et al., 2008) and the MODIS Mosaic of Antarctica (Haran et al., 2013), as a guide to refine the drainage divides. Ice-sheet drainage systems were delineated to identify regions

that are broadly homogeneous regarding surface slope orientation relative to atmospheric advection and denoting the ice-sheet areas feeding large ice shelves. The AP is assigned to four different basins (drainage system ID numbers 24–27), with a relatively clear separation from the ice sheet along 70° S latitude (see Sect. 4.2).

4 Methods

The data generation workflow is roughly divided into four steps: (1) intersecting data sets, (2) defining connectivity levels, (3) calculating glacier-specific attributes (topographic parameters), including ice thickness and volume information, and (4) the calculation of the overall and glacier-specific hypsometry. All calculations are performed with various tools available in ESRI's ArcGIS version 10.2.2. All of the functionality is also available in other geographic information system (GIS) software packages. The four main steps are described in the following sections in more detail.

4.1 Intersecting data sets

When generating an inventory based on the semiautomated band ratio method (Paul et al., 2009), rock outcrops are automatically excluded from the glacier area. In this study the glacier catchment outlines are intersected with the latest vector data set of rock outcrop boundaries from the ADD (see Sect. 3.3). By removing the new rock outcrops from the catchment outlines of Cook et al. (2014), a mask of individual glaciers is generated, assuming that areas not identified since rock outcrops are ice covered. Apart from the rock outcrops, the data set of Cook et al. (2014) is generally in agreement with the procedures and GLIMS guidelines (Racoviteanu et al., 2009; Raup and Khalsa, 2010) for deriving glacier information.

To include glacier-specific ice thickness and volume information, the bedrock grid of Huss and Farinotti (2014) is subtracted from the DEM of Cook et al. (2012) and combined with the new glacier outlines. A grid with ice volume is then derived by multiplying the ice thickness grid with the cell area (10 000 m²).

4.2 Defining connectivity levels

Rastner et al. (2012) suggested that peripheral glaciers on Greenland with a strong dynamic connection to the Greenland Ice Sheet should be regarded as part of the ice sheet and assigned the connectivity level 2 (CL2). This is where glaciers have an extended connection to the ice sheet and the location of their drainage divide on the DEM is uncertain due to the low-sloping terrain. For the Antarctic ice-sheet drainage divides (see Sect. 3.5), basins south of 70° S are strongly connected to the West Antarctic ice sheet. Accordingly, they are assigned CL2 and are not included or further considered in the inventory presented here. The assignment

of CL1 (i.e., weak connectivity to ice sheet) to the glaciers on the mainland and north of 70° S is performed automatically within the GIS following the heritage rule introduced by Rastner et al. (2012), i.e., a glacier connected to a glacier assigned CL1 will also receive the attribute CL1. With this strategy, all glaciers on surrounding islands (i.e., those in the inventory from Bliss et al., 2013) are assigned the value CL0. Large glaciers that are theoretically separable but otherwise closely connected to the ice sheet (e.g., Pine Island and Thwaites) have the value CL2.

4.3 Glacier-specific topographic parameters, ice thickness and volume

All glacier-specific attributes (minimum; maximum; mean; and median elevation; mean slope, aspect, and thickness; total ice volume; and ice volume grounded below sea level) are calculated by combining the glacier outlines with the DEM, the ice thickness and volume grids using the zonal statistics tool in ArcGIS. This tool statistically summarizes the values of the underlying raster data sets (e.g., DEM, ice thickness) within specific zones with a unique ID (glacier outlines) and organizes the results into an attribute table. The table is joined with the attribute table of the glacier outlines data set based on a common and unique identifier in both tables (i.e., the glacier ID). All calculations are performed using the WGS84 South Pole Lambert Azimuthal Equal Area projection.

Since the bedrock and hence also thickness data sets are based, *inter alia*, on the DEM of Cook et al. (2012), they are not universally spatially congruent with the glacier outlines (i.e., the boundary limits differ between the outlines and the other data sets). Of the 1589 glacier outlines, the thickness and volume values could not be calculated for 50 glaciers of the inventory. Accordingly, the topographic parameters, thickness and volume values of the glaciers on the islands that are not completely covered by the ice thickness and bedrock data set do not represent values for complete glaciers. In addition, two glaciers are insufficiently covered by the 100 m × 100 m pixel of the DEM. Hence these glaciers are not or insufficiently covered by the bedrock data set of Huss and Farinotti (2014). Hence, 1541 glaciers have topographic information and 1539 glaciers have thickness, volume and sea level equivalent (SLE) information, of which some only have partial ice thickness and volume information.

To estimate the volume grounded below sea level for each glacier, a grid representing the distribution of the volume grounded below sea level is calculated by extracting the areas of the bedrock grid with negative values (areas below sea level).

The SLE of the ice volume is calculated by assuming a mean ice density of 900 kg m⁻³ (not taking into account firn-air content) and dividing it by the ocean surface area (3.625 × 10⁸ km²; Cogley, 2012), assuming all ice volume contributes to sea level if melted. This is not the case for the grounded ice

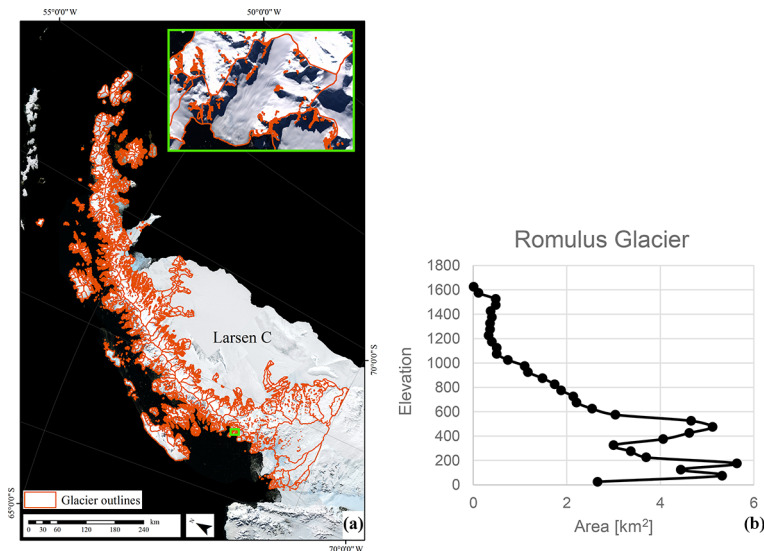


Figure 3. (a) Glacier outlines. Inset map showing Romulus Glacier referred to in Table 2 and (b) exemplifying the glacier-specific hypsometry.

below sea level, which has a negative (lowering) effect since this volume will be replaced by water with a higher density (Cogley et al., 2011). This effect has been considered in a second step in the SLE estimations presented. Other effects, such as the isostatic effect, the cooling and dilution effect on ocean waters by floating ice (Jenkins and Holland, 2007), are not taken into account here.

4.4 Glacier hypsometry

The distribution of the glacierized area with elevation (hypsometry) is calculated (a) for the entire AP in 100 m elevation bins, (b) for the four subregions also in 100 m bins and (c) for each individual glacier using 50 m elevation bins. The calculation is based on the DEM of Cook et al. (2012) that is converted to 100 m bins using the “reclassify” tool and the “extract by mask” tool for the respective subregions. Additionally, the hypsometry of the catchment outlines is calculated to determine the effect of removing rock outcrops from the hypsometry. For further comparisons we also calculated the hypsometry of the marine and ice-shelf-terminating glaciers and the hypsometry of the bedrock.

5 Results

5.1 Size distribution

The glacier inventory for the AP ranges from 63–70° S to 55–70° W and consists of 1589 glaciers covering an area of 95 273 km² (Fig. 3a) without rock outcrops, ice shelves and islands < 0.5 km². Hence, compared to the preexisting data set of Cook et al. (2014), this data set covers a smaller area and one glacier less due to the intersection with the

rock outcrop data set (we removed one glacier since all of its area was rock outcrop). The rock outcrops cover an area of 1709.4 km². The 619 glaciers located on islands (CL0) cover an area of 14 299 km², representing 15 % of the total glacierized area. The remaining 970 glaciers are located on the mainland (CL1), covering 80 974 km² and hence 85 % of the total area. Since the DEM is spatially not perfectly congruent with the glacier outlines, of the total 1589 glacier outlines, 48 outlines do not have any elevation information. As a result, the calculations including the DEM, the bedrock or the thickness data set are only applied to 1541 glaciers, of which some only have partial elevation information. In Table 2 all parameters of the attribute table are listed, including the corresponding values of an example glacier (for location see inset map in Fig. 3a). The hypsometry of each individual glacier, as exemplified in Fig. 3b, is stored and available separately in a csv file. Several parameters, such as primary classification, glacier form and front, and metadata about the satellite image, have been determined and provided by Cook et al. (2014), as defined for the GLIMS inventory. Others (i.e., connectivity levels, topographic parameters, ice thickness and volume) are the result of the calculations described in Sect. 4. The inventory is available for download from the GLIMS website: <http://www.glims.org/maps/glims> (doi:10.7265/N5V98602).

Regarding the connectivity levels, all glaciers on islands surrounding the AP are assigned CL0 (no connection) and the glaciers on the mainland are all assigned CL1 (weak connection). Even the glaciers at the very northern part of the AP have CL1 due to the applied topological heritage rule (a glacier connected to a glacier assigned CL1 also receives CL1). Since the glaciers further south are connected to the ice sheet, they are assigned CL2 (strong connection), are re-

Table 2. Glacier parameters in the attribute table of the inventory of the AP.

Name	Item	Glacier example	Description
Name	Name	Romulus Glacier	String, partially available
Satellite image date	SI_DATE	19.02.2001	Date of the satellite image used for digitizing
Year	SI_YEAR	2001	Year the outline is representing
Satellite image type	SI_TYPE	Landsat 7	Instrument name, e.g., Landsat 7
Satellite image ID	SI_ID	LE7220108000105050	Original ID of image
Coordinates	Lat, long	−68.391218, −66.82767	Decimal degree
Primary classification	Class	6 (mountain glacier)	See Cook et al. (2014)
Form	Form	2 (compound basin)	See Cook et al. (2014)
Front	Front	4 (calving)	See Cook et al. (2014)
Confidence	Confidence	1 Confident about all (class, form and front) classification types	See Cook et al. (2014)
Mainland/island	Mainl_Isl	1 (situated on mainland)	See Cook et al. (2014)
Area	Area	68.9 km ²	km ²
Connectivity level	CL	1 (weak connection)	See Sect. 4.2
Sector	Sector	SW	NW, NE, SW or SE
Minimum elevation	min_elev	4.6 m a.s.l.	m a.s.l.
Maximum elevation	max_elevation	1610.6 m a.s.l.	m a.s.l.
Mean elevation	mean_elev	466.5 m a.s.l.	m a.s.l.
Median elevation	med_elev	425.6 m a.s.l.	m a.s.l.
Mean aspect in degree	mean_asp_d	222°	°
Mean aspect nominal	mean_aspect	SW	Eight cardinal directions
Aspect sector	asp_sector	6	Clockwise numbering of the eight cardinal directions
Mean slope	mean_slope	13°	°
Total volume	tot_vol	13.4 km ³	km ³
Volume below sea level	vol_below	8.0 km ³	km ³
Mean thickness	mean_thick	191.4 m	m

garded as part of the ice sheet and hence are not included in the present data set.

Figure 4a portrays the percentages per size class in terms of number and area. The mean area (60.0 km²) is considerably higher than the median area (8.2 km²), reflecting the areal dominance of a few larger glaciers. Most of the glaciers can be found in the size classes 4–6 (1.0–50 km²). These glaciers account for 77 % of the total number but only for 14 % of the total area. The glaciers larger than 100 km² cover the majority of the area (77 %) yet comprise only 11 % of the total number. With an area of 7018 km², Seller Glacier is the largest, accounting for 7 % of the total area and being twice as large as the second largest glacier (Mercator Ice Piedmont, 3499 km²).

5.2 Topographic parameters

Figure 4b shows the distribution of glacier number and area as a percentage of the total for each aspect sector of the AP. The distribution is rather balanced and does not reveal any trends. Somewhat fewer glaciers and areas have aspects from south to southeast. The large value in area of the southwestern sector derives from the contribution of the largest glacier of the region (Seller Glacier).

Figure 5a and b present a scatter plot of area against mean and median and area against minimum and maximum elevation, revealing that mean, median and maximum elevation increase towards larger glaciers. Three glaciers have a maximum elevation above 3100 m a.s.l., being 300 m or more higher than all other glaciers. The highest elevation is in southern Graham Land with 3172 m. Many glaciers have a minimum elevation of (close to) zero m a.s.l. since most of them are marine terminating. The average mean elevation of the 1541 glaciers with elevation information is 409 m, and their median elevation is 317 m a.s.l. The spatial distribution of median elevation reveals an increase from the coast and islands (0–500 m a.s.l.) to the interior of the AP (up to about 1800 m a.s.l.). This can be seen in Fig. S1 in the Supplement.

When mean aspect is plotted against mean elevation (Fig. 6) there are also no significant trends. However, the highest mean elevation values are lower in the southeastern sector. The scatter plot of mean slope against area (Fig. S2) reveals the common dependence on glacier size, where mean slope decreases towards larger glaciers. Additionally, the scatter is smaller the larger the glacier, indicating that small glaciers exhibit a larger range of slope inclination.

The mean thickness of all 1539 glaciers involving thickness information is 130 m. The Eureka glacier, located in the south, has the largest mean thickness of all CL0 and

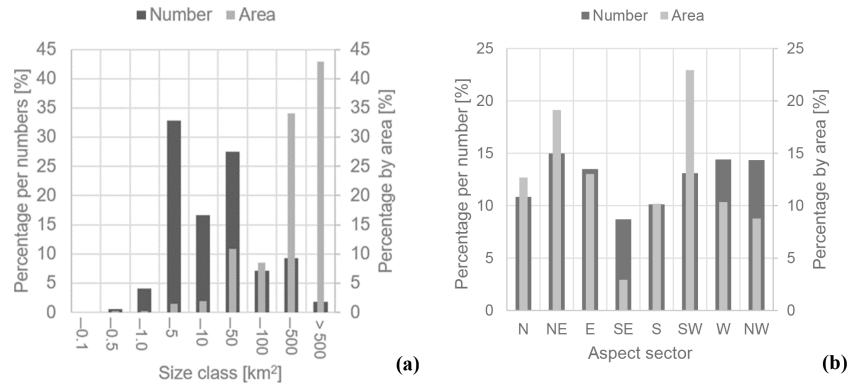


Figure 4. (a) Percentage of glacier count and area per size class (only upper boundary of each size class is given on the *x* axis) and (b) percentage of glacier count and area per aspect sector.

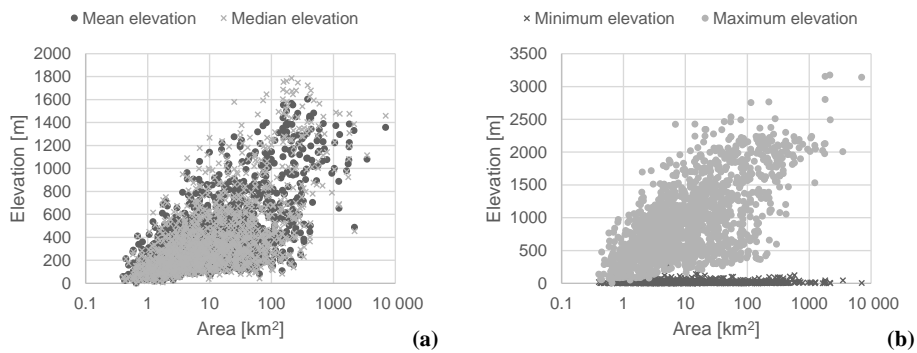


Figure 5. (a) Mean and median elevation vs. area and (b) minimum and maximum elevation vs. area of the 1541 glaciers, including elevation information.

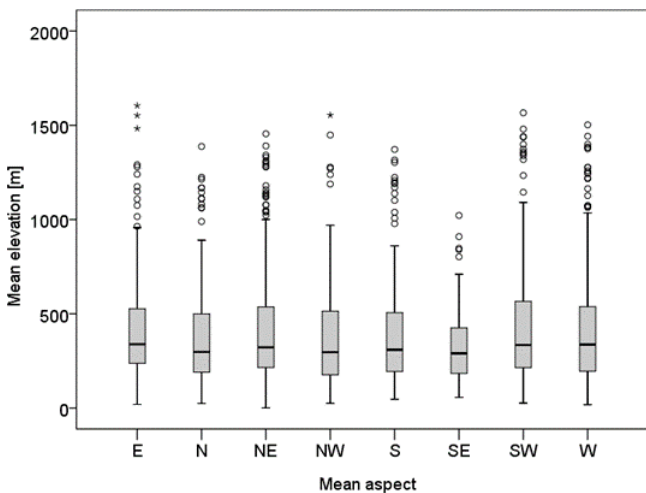


Figure 6. Mean glacier elevation vs. mean glacier aspect of 1541 glaciers. The top and bottom of the boxes indicate the 25th and 75th percentiles, respectively. The whiskers extend to 1.5 times the height of the box and to the minimum values.

CL1 glaciers with 851 m. The dependence of mean thickness on area and slope (indicating that the steeper or smaller the glacier, the thinner the ice) (Fig. 7a, b) is not surprising because ice thickness is modeled based on surface topography (Huss and Farinotti, 2012, 2014). However, low-sloping glaciers reveal a large range of mean thickness values. The large but low-sloping glaciers of the high plateau and those in the very south towards the Antarctic ice sheet form a cluster of glaciers with higher mean thicknesses. The many small glaciers along the coast are mostly thin. The mean thicknesses per sector and per mean aspect (Fig. S3) do not reveal any significant spatial patterns.

The total ice volume of the AP is 34 590 km³. Since the volume is calculated based on the thickness data set, the volume distribution is basically a reflection of the thickness distribution. Table 3 lists the total volume per sector, revealing that most of the ice volume can be found in the southwestern and southeastern sectors (38.6 and 32 % of the total). This is not surprising because these two sectors make up 63 % of the total glacierized area. Regarding the glacier volume per glacier area for individual glaciers, the highest values are found for the large glaciers at the very south of the AP, adja-

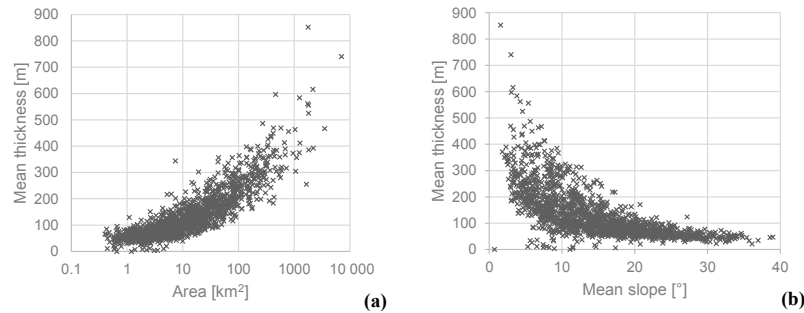


Figure 7. Scatter plot of the 1541 glaciers involving thickness information. **(a)** Mean thickness vs. area and **(b)** mean thickness vs. mean slope.

cent to the ice masses regarded as being a part of the Antarctic ice sheet.

Numerous, partly very pronounced, valleys lie below sea level, especially in the northeastern sector (the bedrock lying below sea level is visualized in Fig. S4). In total, approximately one-third of the total grounded ice volume is below sea level (Table 3), which has a negative effect on SLR (sea level lowering). About 50 % of the volume of the northeastern sector is grounded below sea level (Table 3). Although the negative effect on SLR is very small, this effect can now be better considered for future sea level estimations. Based on the results presented here, this results in a total estimated SLE of 54 mm (Table 3).

As mentioned before, the nominal glacier parameters primary classifications, glacier form and front, have been determined by and described in Cook et al. (2014). They further illustrate the number of glaciers within each classification and frontal type, which is therefore not repeated here.

5.3 Hypsometry

Figure 8a and b depict the glacier hypsometry (area–altitude distribution) for (a) the entire AP and for (b) each sector, revealing a bimodal shape of the hypsometry. Figure 8a additionally displays the hypsometry only for marine-terminating and ice-shelf-nourishing glaciers, as well as the hypsometry of the underlying bedrock. Exclusion of the rock outcrops, with a total area of 1709.4 km², does not change the general shape of the hypsometry. However, it slightly reduces the glacierized areas below 1500 m a.s.l., with a maximum areal reduction at 200–600 m and 1000–1200 m a.s.l. The hypsometry for marine-terminating and ice-shelf-nourishing glaciers confirms that most of the glacierized area is covered by these types. Additionally, these types extend over the entire elevation range. Accordingly, the bimodal shape of the curve does not arise from different glacier (types) at lower and higher elevations. Rather, it is determined by and reflects the topography of the AP: the low-sloping and low-lying coast regions covered by valley glaciers account for the maximum of the glacierized area between approximately 200 and 500 m a.s.l. The glacierized plateau region accounts for a secondary max-

imum at about 1500–1900 m a.s.l. The steep valley walls connecting the plateau with the coastal region result in the minimum at about 800–1400 m a.s.l. In addition, the hypsometry reveals that approximately 6000 km² of the 93 767 km² of glacierized area covered by the DEM is found in the lowest elevation band (0–100 m). These areas are in direct or in close contact with water or ice shelves

The hypsometry per AP sector (Fig. 8b; all excluding rock outcrops) reveals that in the two northern sectors both maxima of the hypsometric curve are less than those of the two southern sectors. The elevations of the maxima are about the same for NW, NE and SW, whereas both maxima of the SE sector are somewhat lower. The glacier cover per sector reflects the bedrock topography of each sector. The bedrock of the northern sectors has less area in the high plateau regions, and therefore most of the glacierized areas are at lower elevations. The southern sectors have a more dominant plateau region favoring more glacierized areas at higher elevations compared to the northern sectors. However, the northeastern sector has the largest fraction of glacierized area in the lowest 100 m and is therefore in direct or in close water or ice shelf contact.

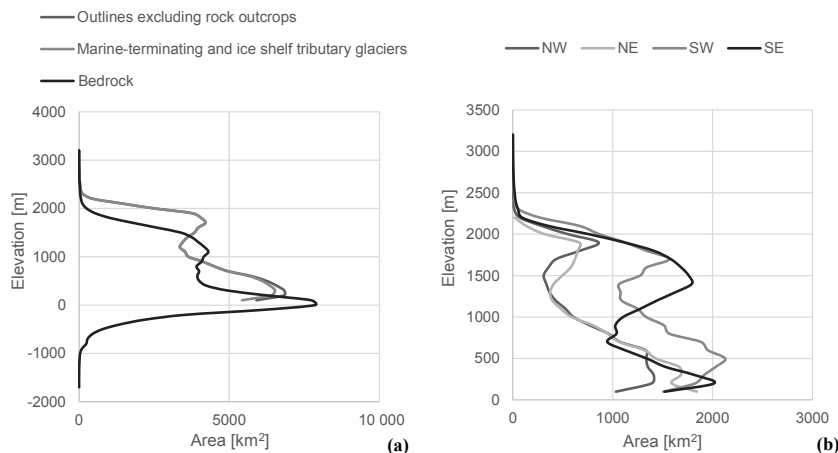
5.4 Discussion

5.5 Source data

This study has presented a complete and now publicly available glacier inventory for the Antarctic Peninsula north of 70° S that has been compiled from the best and most recent preexisting data sets, complemented with information for individual glaciers that was not available before (topographic parameters, hypsography and ice thickness). To allow traceability of source data, we have not altered or corrected the available data sets despite some obvious shortcomings. For example, the DEM by Cook et al. (2012) does not cover all glaciers and covers several only partly, but we have not attempted to fill these missing regions with other source data (e.g., the ASTER GDEM). Consequently, the sample of glaciers with complete attribute information (1539) is reduced compared to the number of all glaciers in the study

Table 3. Glacier number, area, volume, volume grounded below sea level, the corresponding percentages and SLE per sector. For the estimation of SLE, see Sect. 4.3.

Sector	Count	Count with volume info	Area [km ²]	Count [%]	Area [%]	Volume [km ³]	Volume [%]	Volume _{<0} [km ³]	Volume _{<0} [%]	SLE [mm]
NW	704	679	17 218	44	18	4026	12	1093	27	7
NE	246	237	18 278	15	19	6133	18	2939	48	7
SW	378	362	31 130	24	33	13 365	39	4849	36	20
SE	261	261	28 647	17	30	11 065	32	2890	26	20
Total	1589	1539	95 273	100	100	34 590	100	11 771	100	54

**Figure 8.** Glacier hypsometry of the total area covered by the DEM. **(a)** Total areal distribution excluding rock outcrops, areal distribution for marine-terminating and ice-shelf-nourishing glaciers and areal distribution of the underlying bedrock. **(b)** Areal distribution of the glacier cover per sector.

region (1589). The same applies for glaciers with a modeled ice thickness distribution. For 48 of these glaciers, the DEM information was incomplete and ice thickness was accordingly not modeled by Huss and Farinotti (2014). Similarly, for rock outcrops, although the reported accuracy is only $85 \pm 8\%$ and we could identify wrongly classified rock outcrops in comparison to LIMA, we used them as they are. This helps to also be consistent with other studies that will use the same data sets for their purposes. For the same reasons (consistency, traceability), we have also not corrected basin outlines or drainage divides using flow velocity fields derived from satellite sensors because this was also already been done by Cook et al. (2014) for the catchment outlines. Alterations here would also impact the already-existing detailed classification of glacier fronts and we think it is better not to change this at this stage. Overall, results are as good as the source data used and their errors or incompleteness fully propagate into the products we have created here. However, we do not expect any major changes in the glacier characteristics or our overall conclusions with such corrections being implemented. Conversely, addressing the shortcomings and improving the related data sets is certainly an issue to be considered for future work.

5.6 Comparison with other regions

In comparison with other recently compiled glacier inventories in regions of similar environmental conditions (mountainous coastal regions with maritime climate), such as Alaska (Kienholz et al., 2015), Greenland (Rastner et al., 2012) and Svalbard (Nuth et al., 2013), the AP has the largest glacierized area (95 273 km²), closely followed by Greenland (89 720 km²), Alaska (86 723 km²) and with some distance Svalbard (33 775 km²). The AP also has the largest absolute, although only the second largest relative, area covered by marine-terminating glaciers, which are expected to react very sensitively to small changes in climate and associated ocean temperature changes. The glacier number and area distributions in the corresponding studies of Alaska, Greenland, Svalbard and the AP reveal that a few larger glaciers contribute the most to the area in all regions. This dominance is also reflected in a median area, which is considerably smaller than the mean area. However, in Alaska, Greenland and Svalbard the number of small glaciers is distinctively higher, with maximum counts between 0.25 and 1 km². The glaciers of the AP do not exhibit this pattern, which confirms findings by Pfeffer et al. (2014) for glaciers

in the RGI Antarctic and subantarctic regions. Only the glaciers on Svalbard have a favored northern aspect (Nuth et al., 2013), which is interpreted as evidence for the importance of solar radiation incidence for glacier distribution in this region (Evans and Cox, 2010).

The bimodal hypsometric curve for the glaciers on the AP (Fig. 8) is very important compared to the parabolic shape of the three other regions that have increasing area percentages towards their mid-elevation. Hence, the AP has most of its glacierized area at lower elevations (around 200–500 m), with a secondary peak at higher elevations (around 1500–1900 m). Since the hypsometry of a glacier is an indicator of its climatic sensitivity (Jiskoot et al., 2009), this comparison reveals that the future evolution of AP glaciers cannot be modeled with the same simplified approaches as glaciers in other regions (Raper et al., 2000) and that volume loss for a small rise in the equilibrium line altitude (ELA) might indeed be high (Hock et al., 2009). The aspect preference with poleward tendencies of glacier distribution that is common in other mountain ranges (Evans, 2006, 2007; Evans and Cox, 2005, 2010) could not be found for the AP because the entire AP is glacierized and most glaciers are marine terminating.

5.7 Uncertainties

5.7.1 Impacts on outlines and meta-information

A wide range of interconnected uncertainties impact the glacier outlines and the associated meta-information. Since we have taken data sets from the literature as they are, we restrict the analysis of uncertainties to the information reported in the related studies (see Sect. 5.7.2) and add here a more generalized description of the respective impacts. *Glacier outlines* are composed of (A) the outlines from LIMA, (B) the drainage divides from Cook et al. (2014) and (C) the rock outcrop data set by Burton-Johnson et al. (2016). Key factors influencing their accuracy are related to (A1) grounding line position (only for glaciers merging with ice shelves), (A2) accuracy of the digitizing, (B1) the accuracy of the DEM from Cook et al. (2012), (C1) correct mapping (yes or no) and (C2) positional accuracy of the rock outcrops. Whereas the impact of (A2) and (C2) on the derived glacier areas is small since deviations are generally normally distributed (i.e., they only impact precision), impacts of (A1) and (B1) on glacier area can be large. However, for (B1) the impact is mostly on the size class distribution of the glaciers since a shift of an internal drainage divide does not change the total area. Factor (C1) might have a larger impact on smaller glaciers (i.e., a missed rock outcrop can increase glacier area by 5 % or more), but for most of the larger glaciers the area overestimation will be less than 1 or 2 %. Therefore, the largest impact on glacier area comes from source (A1), albeit only for a subsample (264) of glaciers merging with ice shelves.

The accuracy of the meta-information provided with each glacier (topographic parameters, ice thickness) depends on (D) the DEM used to calculate them, (E) the bedrock data set by Huss and Farinotti (2012) and (F) the glacier outlines that provide the perimeter for the calculation. For these sources we can identify the following impacts: (D1) a glacier is not or only partly covered by DEM information, (D2) the parameter is more or less impacted by DEM accuracy, (E1) there is direct propagation of DEM accuracy (slope) into the ice thickness calculation, (E2) there is missing consideration of rock outcrops (C) in (E), and (F1) changes of the meta-information due to errors in the extent. For the latter (F1), one can expect under- or overestimation of mean slope in case of a grounding line being too extensive (resulting in more area with small slopes) or rock outcrops in steep terrain having been missed (resulting in more area with steep slopes). Positional uncertainty will impact all topographic parameters, but very likely not systematically (i.e., not resulting in a bias) since terrain differences should average out. Uncertainty source (E1) is highly variable and discussed by Huss and Farinotti (2012), and (E2) causes inconsistencies among the derived glacier volumes, but overall differences are likely small since they are not systematic. Glaciers not covered by DEM cells (D1) have simply no data, but for those partly covered, the existing DEM cells have been used for the calculation. Depending on the coverage, results might still be useful, but in general it might be better to also set them to no data to avoid misinterpretation. Finally, the impact of (D2) will vary with the parameter. These parameters calculated from individual cells (e.g., minimum or maximum elevation) will be more strongly influenced by DEM errors or artifacts than those based on aggregate numbers such as mean or median elevation (Frey and Paul, 2012). A quantitative assessment of the related impacts can only be performed once a better DEM is available for the region. So far, the manually corrected DEM from Cook et al. (2012) is likely the best data set available.

5.7.2 Input data uncertainties

The uncertainties for the input data sets used are given as follows. The positional accuracy of the grounding line varies strongly with the nature of the boundary and is given as ± 502 m for the outlet glacier boundaries merging with ice shelves (Bindschadler et al., 2011). For the outline positions of other glaciers, an uncertainty of ± 2 pixel (30 m) is assumed. The classification of rock outcrops is based on an automated but manually checked classification. The mean value for correct pixel identification is given as 85 ± 8 % (Burton-Johnson et al., 2016). The application of the DEM causes uncertainties in drainage divides and topographic parameters. According to Cook et al. (2012), the accuracy of the DEM is < 200 m horizontally and about ± 25 m vertically, but it varies regionally. Large shifts of the outlines in flat terrain are thus possible, causing the highly variable impacts on glacier

area as described before. The impact of DEM uncertainties on topographic parameters is higher for smaller glaciers and those depending on single-cell values. Given our experiences with other DEMs, we estimate the uncertainty to be ± 50 m for all elevations and $\pm 5^\circ$ for mean slope and aspect. For the regionally varying uncertainty of thickness and the corresponding uncertainty in volume and SLE, we refer to the detailed estimates of Huss and Farinotti (2012).

5.7.3 Further comments on the input data sets

The DEM of Cook et al. (2012) currently provides the highest resolution and quality for the area of the AP. However, the DEM only covers 93 250 km² and hence 98.4 % of the total glacierized area. In consequence, the calculation of the topographic parameters (mean, median, minimum and maximum elevation, slope, aspect) was not possible for 48 glaciers, representing an area of 1044 km², or 3 % (1 %) of the total number (area). For example, the region of Renaud and Bischoe islands at the midwestern coast of the AP does not have any elevation information. As some glaciers are only partially covered by the DEM, their parameters are likely based on a nonrepresentative part of the glacier. Moreover, glacier hypsometry is calculated based on the DEM and represents only the area covered by the DEM. Since the ice thickness and bedrock data set of Huss and Farinotti (2014) is also based on the DEM of Cook et al. (2012), mean thickness and volume could not be calculated for 50 glaciers. We suggest adding the now missing topographic information as soon as these glaciers are covered by a DEM of appropriate quality (e.g., the forthcoming TanDEM-X DEM). This new DEM might also then be used to recalculate drainage divides, grounding lines, glacier extents and ice thickness distribution considering the improved rock outcrop data set. This would also help to overcome the current inconsistencies among the applied data sets.

The new rock outcrop data set already has a higher accuracy and is more consistent than the former data set provided by the ADD. However, as mentioned above, some areas are still misclassified and an in-depth check and correction for the glaciers on the AP would help further improve the new inventory. Conversely, manual correction of these errors for the entire region would remove the traceability to the source data sets and we decided to maintain it for this first version.

To divide the glaciers from ice shelves, Cook et al. (2014) used the grounding line based on the ASAD project data source (Bindschadler et al., 2011), modified in places with features visible in the LIMA. Because the definition of the location of the grounding line significantly influences the extent of a glacier flowing into an ice shelf, grounding line positions obtained from new and forthcoming techniques will also alter glacier extent. However, this is then more a matter of definition rather than uncertainty.

5.8 Assignment of connectivity levels

In the south, the assignment of connectivity levels corresponds with the Antarctic ice-sheet drainage divides from the Cryosphere Science Laboratory of NASA's Earth Sciences Divisions (Zwally et al., 2012), which has assigned all unconnected glaciers (on islands) a CL0 and all glaciers on the AP CL1, following the suggestion by Rastner et al. (2012) for peripheral glaciers on Greenland. It is certainly the simplest possibility for such an assignment, but we think it is nevertheless sensible and fulfils its purpose. Consistency with earlier applications (e.g., all glaciers in the inventory by Bliss et al., 2013 have CL0) and transparency of the method are further benefits. It also allows the glacier and ice-sheet measuring and modeling communities to perform their work with their respective methods and determine, for example, past or future mass loss and/or sea level contributions independently. This would allow a cross check of methods for individual glaciers that are not resolved (such as results from gravimetry and glacier models) and possibly also explain remaining differences between methods (Shepherd et al., 2012; Briggs et al., 2017). The problem of double counting the contributions can also be avoided.

5.9 Specific characteristics of the AP glaciers

The ELA for a balanced budget (ELA₀) of land-terminating glaciers can be well approximated from topographic indices such as the mean, median or midpoint elevation (e.g., Braithwaite and Raper, 2009). The ELA is also a good proxy for precipitation (Ohmura, 1992; Oerlemans, 2005) and useful for modeling the effect of rising temperatures on future glacier extent (Zemp et al., 2006, 2007; Paul et al., 2007; Cogley et al., 2011;). However, since the glaciers of the AP are mainly marine-terminating glaciers (Vaughan et al., 2013), the lower limits of these glaciers are predefined and the ELA variability is largely determined by the variability of the topography (i.e., its maximum elevation). The increasing median elevation towards the interior (Fig. S1) does not result from decreasing precipitation towards the interior but is a consequence of glacier hypsometry and depends on whether a glacier reaches sea level or not.

The bimodal shape of the hypsometry, revealing that half of the glacierized areas are situated below 800 m a.s.l., as well as the high areal fraction of marine-terminating glaciers, indicates a high sensitivity of the AP glaciers to rising air and water temperatures (Hock et al., 2009). Due to their special hypsometry, their sensitivity is likely higher than for glaciers in Alaska, Greenland or Svalbard since these have a smaller fraction of marine-terminating glaciers and a smaller share of area at very low elevations.

The total ice volume and the volume below sea level are necessary for accurate estimations of the sea level contribution. At 54 mm the AP's glaciers have a higher contribution potential than the glaciers of Alaska (45 mm), Central Asia

(10 mm), the Greenland periphery (38 mm), the Russian Arctic (31 mm) or Svalbard (20 mm) (Huss and Hock, 2015). In total, global glaciers have a potential SLR of approximately 374 mm (Huss and Hock, 2015) to 500 mm (Huss and Farinotti, 2012; Vaughan et al., 2013), which is still significant for low-lying coastal regions (Paul, 2011; Marzeion and Levermann, 2014). Compared to the Antarctic ice sheet, with a SLE of 58.3 m (Vaughan et al., 2013), the SLE of the AP seems negligible. However, regarding the high sensitivity and much shorter response times of these glaciers to climate change, they are expected to be major contributors to SLR in the next decades (Hock et al., 2009). As the contribution of the AP's glaciers has not yet been fully considered in most studies, the new inventory can now be used to model their evolution explicitly with the current best approaches (e.g., Huss and Hock, 2015).

The results presented here allow a rough approximation of the consequences of ongoing climate change for the AP: with respect to the hypsometry, the lowest 800 m and hence 50 % of the glacierized area is prone to rising ablation and mass loss, causing a sea level contribution of roughly 50 % of the total AP SLE (27 mm). Regarding the glacier termini, about 30 % of the glacierized areas flow into the Larsen C ice shelf. Collapse of this ice shelf (similar to Larsen A and B), which may happen soon due to a growing rift (Jansen et al., 2015), would likely cause rapid dynamic thinning of its tributary glaciers (e.g., Rott et al., 2011) due to debuttressing. About 15 % of the SLE (9 mm) from the lowest 800 m is attached to the Larsen C ice shelf.

6 Data availability

The present inventory is available from the GLIMS database at doi:10.7265/N5V98602. Table 1 gives an overview of the data sets used for the generation of the inventory and their sources.

7 Conclusions

The compilation of a glacier inventory of the AP (63–70° S, Graham Land), consisting of glacier outlines accompanied by glacier-specific parameters, was achieved by combining already existing data sets with GIS techniques. The exclusion of rock outcrops by using the latest corresponding data set of the ADD (Burton-Johnson et al., 2016) from the glacier catchment outlines of Cook et al. (2014) resulted in 1589 glacier outlines (excluding ice shelves and islands < 0.5 km²), covering an area of 95 273 km². Combining the outlines with the DEM of Cook et al. (2012) enabled us to derive several topographic parameters for each glacier. By applying the bedrock data set of Huss and Farinotti (2014), volume and mean thickness information was calculated for each glacier.

Connectivity levels with the ice sheet were assigned to all glaciers following Rastner et al. (2012) to facilitate observations and modeling by different groups. We started with a simple and transparent rule: glaciers south of 70° S (Palmer Land) are assigned CL2 and are regarded as being part of the ice sheet, while all glaciers north of it and on the AP are assigned CL1 and all glaciers on surrounding islands are assigned CL0. The resulting inventory and its quality are largely influenced by the availability and accessibility of accurate auxiliary data sets. For instance, the DEM does only cover 98.4 % of the glacierized area. Hence, for 50 glaciers the topographic parameters, thickness and volume information are missing. For other glaciers, the values are not representative for the entire glacier because smaller parts have no DEM information. Future improved DEMs might help completely cover these glaciers.

Since GLIMS now provides the complete glacier outlines data set of the AP (see glims.org), a significant gap in the global glacier inventory has been closed and a major contribution for forthcoming regional and global glaciological investigations can be made. Furthermore, the new inventory demonstrates the potential for improving knowledge about glacier characteristics, sensitivities and similarities and differences to glaciers in other regions. With the full inventory now freely available, approaches to improving, extending and further investigating the glaciers of the AP are strongly encouraged.

The Supplement related to this article is available online at doi:10.5194/essd-9-115-2017-supplement.

Author contributions. Jacqueline Huber compiled and analyzed this data set in the framework of a master's thesis and prepared the manuscript. Frank Paul and Michael Zemp supervised the thesis and helped with the preparation of the manuscript. Alison J. Cook generated the glacier catchment data set and provided this data set, including information about the generation process.

Competing interests. The authors declare that they have no conflict of interest.

Acknowledgements. Jacqueline Huber and Michael Zemp acknowledge financial support by the Swiss GCOS at the Federal Office of Meteorology and Climatology MeteoSwiss. The work of Frank Paul is funded by the ESA project *Glaciers_cci* (4000109873/14/I-NB). We are grateful to the LIMA Project, the Antarctic Digital Database and the National Snow and Ice Data Center and The Cryosphere Science Laboratory of NASA's Earth Sciences Divisions for free download of their data, allowing us to realize this study. We would also like to thank Matthias Huss

and Daniel Farinotti for making their ice thickness data available as well as for their practical input. The inventory and the study benefited greatly from their bedrock data set. Finally, we would like to thank R. Drews, B. Marzeion and the anonymous referee for the constructive suggestions for improving the quality of this paper.

Edited by: R. Drews

Reviewed by: B. Marzeion and one anonymous referee

References

- ADD Consortium: Antarctic Digital Database, Version 6.0, available at: <http://add.scar.org/home/add6>, last access: 4 May 2015, 2012.
- Arendt, A., Bolch, T., Cogley, J. G., Gardner, A., Hagen, J.-O., Hock, R., Kaser, G., Pfeffer, W. T., Moholdt, G., Paul, F., Radić, V., Andreassen, M., Bajracharya, S., Beedle, M. J., Berthier, E., Bhabri, R., Bliss, A., Brown, I., Burgess, D. O., Burgess, E. W., Cawkwell, F., Chinn, T., Copland, L., Davies, B., de Angelis, H., Dolgova, H., Filbert, K., Forester, R., Fountain, A., Frey, H., Giffen, B., Glasser, N., Gurney, S., Hagg, W., Hall, D., Haritashya, U. K., Hartmann, G., Helm, C., Herreid, S., Howat, I. M., Kapustin, G., Khromova, T., Kienholz, C., Koenig, M., Kohler, J., Kriegel, D., Kutuzov, S., Lavrentiev, I., Le Bris, R., Lund, J., Manley, W. F., Mayer, C., Miles, E. S., Li, X., Menounos, B., Mercer, A., Mölg, N., Mool, P., Nosenko, G., Negrete, A., Nuth, C., Pettersson, R., Racoviteanu, A., Ranzi, R., Rastner, P., Rau, F., Raup, B. H., Rich, J., Rott, H., Schneider, C., Seliverstov, Y., Sharp, M. J., Sigurosson, O., Stokes, C. R., Wheate, R., Wolken, G. J., Wyatt, F., and Zheltyhina, N.: Randolph Glacier Inventory – A Dataset of Global Glacier Outlines: Version 5.0, Global Land Ice Measurements from Space, Boulder CO, USA, 2015.
- Arigony-Neto, J., Skvarca, P., Marinsek, S., Braun, M., Humbert, A., Júnior, C. W. M., and Jaña, R.: Monitoring Glacier Changes on the Antarctic Peninsula, in: *Global Land Ice Measurements from Space*, edited by: Kargel, J. S., Leonard, G. J., Bishop, M. P., Kääh, A., and Raup, B. H., Springer Berlin Heidelberg, Berlin, Heidelberg, 717–741, doi:10.1007/978-3-540-79818-7_30, 2014.
- Bindschadler, R., Vornberger, P., Fleming, A. H., Fox, A. J., Mullins, J., Binnie, D., Paulsen, S. J., Granne-man, B., and Gorodetzky, D.: The Landsat Image Mosaic of Antarctica, *Remote Sens. Environ.*, 112, 4214–4226, doi:10.1016/j.rse.2008.07.006, 2008.
- Bindschadler, R., Choi, H., Wichlacz, A., Bingham, R., Bohlander, J., Brunt, K., Corr, H., Drews, R., Fricker, H., Hall, M., Hindmarsh, R., Kohler, J., Padman, L., Rack, W., Rotschky, G., Urbini, S., Vornberger, P., and Young, N.: Getting around Antarctica: new high-resolution mappings of the grounded and freely-floating boundaries of the Antarctic ice sheet created for the International Polar Year, *The Cryosphere*, 5, 569–588, doi:10.5194/tc-5-569-2011, 2011.
- Bliss, A., Hock, R., and Cogley, J. G.: A new inventory of mountain glaciers and ice caps for the Antarctic periphery, *Ann. Glaciol.*, 54, 191–199, doi:10.3189/2013AoG63A377, 2013.
- Bolch, T., Menounos, B., and Wheate, R.: Landsat-based inventory of glaciers in western Canada, 1985–2005, *Remote Sens. Environ.*, 114, 127–137, doi:10.1016/j.rse.2009.08.015, 2010.
- Braithwaite, R. J. and Raper, S.: Estimating equilibrium-line altitude (ELA) from glacier inventory data, *Ann. Glaciol.*, 50, 127–132, doi:10.3189/172756410790595930, 2009.
- Briggs, K. H., Shepherd, A., Muir, A., Gilbert, L., McMillan, M., Paul, F., and Bolch, T.: Sustained high rates of mass loss from Greenland's glaciers and ice caps, *Geophys. Res. Lett.*, submitted, 2017.
- Burton-Johnson, A., Black, M., Fretwell, P. T., and Kaluza-Gilbert, J.: An automated methodology for differentiating rock from snow, clouds and sea in Antarctica from Landsat 8 imagery: a new rock outcrop map and area estimation for the entire Antarctic continent, *The Cryosphere*, 10, 1665–1677, doi:10.5194/tc-10-1665-2016, 2016.
- Cogley, J. G.: Area of the Ocean, *Mar. Geod.*, 35, 379–388, doi:10.1080/01490419.2012.709476, 2012.
- Cogley, J. G., Hock, R., Rasmussen, L. A., Arendt, A. A., Bauder, A., Braithwaite, R. J., Jansson, P., Kaser, G., Möller, M., Nicholson, L., and Zemp, M.: Glossary of glacier mass balance and related terms, Technical documents in hydrology, IHP-VII, No. 86, UNESCO, Paris, France, vi, 114, doi:10.1657/1938-4246-44.2.256b, 2011.
- Cook, A. J., Murray, T., Luckman, A., Vaughan, D. G., and Bar- rand, N. E.: A new 100-m Digital Elevation Model of the Antarctic Peninsula derived from ASTER Global DEM: methods and accuracy assessment, *Earth Syst. Sci. Data*, 4, 129–142, doi:10.5194/essd-4-129-2012, 2012.
- Cook, A. J., Vaughan, D. G., Luckman, A. J., and Murray, T.: A new Antarctic Peninsula glacier basin inventory and observed area changes since the 1940s, *Antarct. Sci.*, 26, 614–624, doi:10.1017/S0954102014000200, 2014.
- Cook, A. J., Holland, P. R., Meredith, M. P., Murray, T., Luckman, A., and Vaughan, D. G.: Ocean forcing of glacier retreat in the western Antarctic Peninsula, *Science*, 353, 283–286, doi:10.1126/science.aae0017, 2016.
- Davies, B. J., Hambrey, M. J., Smellie, J. L., Carrivick, J. L., and Glasser, N. F.: Antarctic Peninsula Ice Sheet evolution during the Cenozoic Era, *Quaternary Sci. Rev.*, 31, 30–66, doi:10.1016/j.quascirev.2011.10.012, 2012.
- DiMarzio, J. P.: GLAS/ICESat 500 m Laser Altimetry Digital Elevation Model of Antarctica, 1st Edn., National Snow and Ice Data Center (NSIDC), Boulder, Colorado USA, doi:10.5067/K2IMI0L24BRJ, 2007.
- Evans, I. S.: Local aspect asymmetry of mountain glaciation: A global survey of consistency of favoured directions for glacier numbers and altitudes, *Geomorphology*, 73, 166–184, doi:10.1016/j.geomorph.2005.07.009, 2006.
- Evans, I. S.: Glacier distribution and direction in the Arctic: The unusual nature of Svalbard, *Landform Analysis*, 5, 21–24, 2007.
- Evans, I. S. and Cox, N. J.: Global variations of local asymmetry in glacier altitude: Separation of north–south and east–west components, *J. Glaciol.*, 51, 469–482, doi:10.3189/172756505781829205, 2005.
- Evans, I. S. and Cox, N. J.: Climatogenic north–south asymmetry of local glaciers in Spitsbergen and other parts of the Arctic, *Ann. Glaciol.*, 51, 16–22, doi:10.3189/172756410791392682, 2010.
- Fretwell, P., Pritchard, H. D., Vaughan, D. G., Bamber, J. L., Bar- rand, N. E., Bell, R., Bianchi, C., Bingham, R. G., Blankenship, D. D., Casassa, G., Catania, G., Callens, D., Conway, H., Cook, A. J., Corr, H. F. J., Damaske, D., Damm, V., Ferraccioli, F., Fors-

- berg, R., Fujita, S., Gim, Y., Gogineni, P., Griggs, J. A., Hindmarsh, R. C. A., Holmlund, P., Holt, J. W., Jacobel, R. W., Jenkins, A., Jokat, W., Jordan, T., King, E. C., Kohler, J., Krabill, W., Riger-Kusk, M., Langley, K. A., Leitchenkov, G., Leuschen, C., Luyendyk, B. P., Matsuoka, K., Mouginot, J., Nitsche, F. O., Nogi, Y., Nost, O. A., Popov, S. V., Rignot, E., Rippin, D. M., Rivera, A., Roberts, J., Ross, N., Siegert, M. J., Smith, A. M., Steinhage, D., Studinger, M., Sun, B., Tinto, B. K., Welch, B. C., Wilson, D., Young, D. A., Xiangbin, C., and Zirizzotti, A.: Bedmap2: improved ice bed, surface and thickness datasets for Antarctica, *The Cryosphere*, 7, 375–393, doi:10.5194/tc-7-375-2013, 2013.
- Frey, H. and Paul, F.: On the suitability of the SRTM DEM and ASTER GDEM for the compilation of topographic parameters in glacier inventories, *Int. J. Appl. Earth Obs.*, 18, 480–490, doi:10.1016/j.jag.2011.09.020, 2012.
- GLIMS and NSIDC: Global Land Ice Measurements from Space glacier database, Compiled and made available by the international GLIMS community and the National Snow and Ice Data Center, Boulder CO, USA, doi:10.7265/N5V98602, 2005, updated 2016.
- Haran, T., Bohlander, J., Scambos, T., Painter, T., and Fahnestock, M.: MODIS Mosaic of Antarctica 2003–2004 (MOA2004), NSIDC: National Snow and Ice Data Center, Boulder Colorado, USA, doi:10.7265/N5ZK5DM5, 2005, updated 2013.
- Helm, V., Humbert, A., and Miller, H.: Elevation and elevation change of Greenland and Antarctica derived from CryoSat-2, *The Cryosphere*, 8, 1539–1559, doi:10.5194/tc-8-1539-2014, 2014.
- Hock, R., de Woul, M., Radić, V., and Dyurgerov, M.: Mountain glaciers and ice caps around Antarctica make a large sea-level rise contribution, *Geophys. Res. Lett.*, 36, L07501, doi:10.1029/2008GL037020, 2009.
- Hulbe, C. L., Scambos, T. A., Youngberg, T., and Lamb, A. K.: Patterns of glacier response to disintegration of the Larsen B ice shelf, Antarctic Peninsula, *Global Planet. Change*, 63, 1–8, doi:10.1016/j.gloplacha.2008.04.001, 2008.
- Huss, M. and Farinotti, D.: Distributed ice thickness and volume of all glaciers around the globe, *J. Geophys. Res.*, 117, F04010, doi:10.1029/2012JF002523, 2012.
- Huss, M. and Farinotti, D.: A high-resolution bedrock map for the Antarctic Peninsula, *The Cryosphere*, 8, 1261–1273, doi:10.5194/tc-8-1261-2014, 2014.
- Huss, M. and Hock, R.: A new model for global glacier change and sea-level rise, *Front. Earth Sci.*, 3, 382, doi:10.3389/feart.2015.00054, 2015.
- Jansen, D., Luckman, A. J., Cook, A., Bevan, S., Kulesa, B., Hubbard, B., and Holland, P. R.: Brief Communication: Newly developing rift in Larsen C Ice Shelf presents significant risk to stability, *The Cryosphere*, 9, 1223–1227, doi:10.5194/tc-9-1223-2015, 2015.
- Jenkins, A. and Holland, D.: Melting of floating ice and sea level rise, *Geophys. Res. Lett.*, 34, L16609, doi:10.1029/2007GL030784, 2007.
- Jiskoot, H., Curran, C. J., Tessler, D. L., and Shenton, L. R.: Changes in Clemenceau Icefield and Chaba Group glaciers, Canada, related to hypsometry, tributary detachment, length-slope and area-aspect relations, *Ann. Glaciol.*, 50, 133–143, doi:10.3189/172756410790595796, 2009.
- Kienholz, C., Herreid, S., Rich, J. L., Arendt, A. A., Hock, R., and Burgess, E. W.: Derivation and analysis of a complete modern-date glacier inventory for Alaska and northwest Canada, *J. Glaciol.*, 61, 403–420, doi:10.3189/2015JoG14J230, 2015.
- Kienholz, C., Hock, R., and Arendt, A. A.: A new semi-automatic approach for dividing glacier complexes into individual glaciers, *J. Glaciol.*, 59, 925–937, doi:10.3189/2013JoG12J138, 2013.
- Kunz, M., King, M. A., Mills, J. P., Miller, P. E., Fox, A. J., Vaughan, D. G., and Marsh, S. H.: Multi-decadal glacier surface lowering in the Antarctic Peninsula, *Geophys. Res. Lett.*, 39, L19502, doi:10.1029/2012GL052823, 2012.
- Marzeion, B. and Levermann, A.: Loss of cultural world heritage and currently inhabited places to sea-level rise, *Environ. Res. Lett.*, 9, 034001, doi:10.1088/1748-9326/9/3/034001, 2014.
- Nuth, C., Kohler, J., König, M., von Deschanden, A., Hagen, J. O., Kääh, A., Moholdt, G., and Pettersson, R.: Decadal changes from a multi-temporal glacier inventory of Svalbard, *The Cryosphere*, 7, 1603–1621, doi:10.5194/tc-7-1603-2013, 2013.
- Oerlemans, J.: Extracting a climate signal from 169 glacier records, *Science*, 308, 675–677, doi:10.1126/science.1107046, 2005.
- Ohmura, A.: Energy and mass balance during the melt season at the equilibrium line altitude, Paakitsoq, Greenland Ice Sheet (69°34′25.3″ North, 49°17′44.1″ West, 1155 M A.S.L.), ETH Greenland Expedition Progress Report No. 2, Dept of Geography, ETH Zürich, 94 pp., 1992.
- Paul, F.: Sea-level rise: Melting glaciers and ice caps, *Nat. Geosci.*, 4, 71–72, doi:10.1038/ngeo1074, 2011.
- Paul, F., Kääh, A., Maisch, M., Kellenberger, T., and Haeberli, W.: The new remote-sensing-derived Swiss glacier inventory: I. Methods, *Ann. Glaciol.*, 34, 355–361, doi:10.3189/172756402781817941, 2002.
- Paul, F., Maisch, M., Rothenbühler, C., Hoelzle, M., and Haeberli, W.: Calculation and visualisation of future glacier extent in the Swiss Alps by means of hypsographic modelling, *Global Planet. Change*, 55, 343–357, doi:10.1016/j.gloplacha.2006.08.003, 2007.
- Paul, F., Barry, R. G., Cogley, J. G., Frey, H., Haeberli, W., Ohmura, A., Ommann, C., Raup, B., Rivera, A., and Zemp, M.: Recommendations for the compilation of glacier inventory data from digital sources, *Ann. Glaciol.*, 50, 119–126, doi:10.3189/172756410790595778, 2009.
- Pfeffer, W. T., Arendt, A. A., Bliss, A., Bolch, T., Cogley, J. G., Gardner, A. S., Hagen, J.-O., Hock, R., Kaser, G., Kienholz, C., Miles, E. S., Moholdt, G., Mölg, N., Paul, F., Radić, V., Rastner, P., Raup, B. H., Rich, J., and Sharp, M. J.: The Randolph Glacier Inventory: a globally complete inventory of glaciers, *J. Glaciol.*, 60, 537–552, doi:10.3189/2014JoG13J176, 2014.
- Pritchard, H. D. and Vaughan, D. G.: Widespread acceleration of tidewater glaciers on the Antarctic Peninsula, *J. Geophys. Res.*, 112, F03S29, doi:10.1029/2006JF000597, 2007.
- Racoviteanu, A. E., Paul, F., Raup, B., Khalsa, S. J. S., and Armstrong, R.: Challenges and recommendations in mapping of glacier parameters from space: results of the 2008 Global Land Ice Measurements from Space (GLIMS) workshop, Boulder, Colorado, USA, *Ann. Glaciol.*, 50, 53–69, doi:10.3189/172756410790595804, 2009.
- Raper, S. C. B., Brown, O., and Braithwaite, R. J.: A geometric glacier model for sea-level change calculations, *J. Glaciol.*, 46, 357–368, doi:10.3189/172756500781833034, 2000.

- Rastner, P., Bolch, T., Mölg, N., Machguth, H., Le Bris, R., and Paul, F.: The first complete inventory of the local glaciers and ice caps on Greenland, *The Cryosphere*, 6, 1483–1495, doi:10.5194/tc-6-1483-2012, 2012.
- Rau, F., Mauz, F., Vogt, S., Khalsa, S. J. S., and Raup, B.: Illustrated GLIMS glacier classification manual: glacier classification guidance for the GLIMS inventory, Version 1, available at: www.glims.org/MapsAndDocs/guides.html, last access: 7 January 2016, 2005.
- Raup, B. and Khalsa, S. J. S.: GLIMS Analysis Tutorial, available at: www.glims.org/MapsAndDocs/guides.html, last access: 7 January 2016, 2010.
- Rignot, E. and Thomas, R. H.: Mass balance of polar ice sheets, *Science*, 297, 1502–1506, doi:10.1126/science.1073888, 2002.
- Rignot, E., Mouginot, J., and Scheuchl, B.: Antarctic grounding line mapping from differential satellite radar interferometry, *Geophys. Res. Lett.*, 38, L10504, doi:10.1029/2011GL047109, 2011.
- Rott, H., Skvarca, P., and Nagler, T.: Rapid Collapse of Northern Larsen Ice Shelf, Antarctica, *Science*, 271, 788–792, doi:10.1126/science.271.5250.788, 1996.
- Rott, H., Müller, F., Nagler, T., and Floricioiu, D.: The imbalance of glaciers after disintegration of Larsen-B ice shelf, Antarctic Peninsula, *The Cryosphere*, 5, 125–134, doi:10.5194/tc-5-125-2011, 2011.
- Shepherd, A., Wingham, D., Payne, T., and Skvarca, P.: Larsen ice shelf has progressively thinned, *Science*, 302, 856–859, doi:10.1126/science.1089768, 2003.
- Shepherd, A., Ivins, E. R., A, G., Barletta, V. R., Bentley, M. J., Bettadpur, S., Briggs, K. H., Bromwich, D. H., Forsberg, R., Galin, N., Horwath, M., Jacobs, S., Joughin, I., King, M. A., Lenaerts, J. T. M., Li, J., Ligtenberg, S. R. M., Luckman, A., Luthcke, S. B., McMillan, M., Meister, R., Milne, G., Mouginot, J., Muir, A., Nicolas, J. P., Paden, J., Payne, A. J., Pritchard, H., Rignot, E., Rott, H., Sorensen, L. S., Scambos, T. A., Scheuchl, B., Schrama, E. J. O., Smith, B., Sundal, A. V., van Angelen, J. H., van de Berg, W. J., van den Broeke, M. R., Vaughan, D. G., Velicogna, I., Wahr, J., Whitehouse, P. L., Wingham, D. J., Yi, D., Young, D., and Zwally, H. J.: A Reconciled Estimate of Ice-Sheet Mass Balance, *Science*, 338, 1183–1189, doi:10.1126/science.1228102, 2012.
- Turner, J., Bindschadler, R., Convey, P., DiPrisco, G., Fahrbach, E., Gutt, J., Hodgson, D., Mayewski, P., and Summerhayes, C.: Antarctic Climate Change and the Environment. A contribution to the International Polar Year 2007–2008, Scientific Committee on Antarctic Research, Cambridge, 526 pp., 2009.
- UNESCO: Combined Heat, Ice and Water Balances at Selected Glacier Basins – A contribution to the International Hydrological Decade – A guide for compilation and assemblage of data for glacier mass balance measurements, UNESCO Technical papers in hydrology, 5, 35 pp., 1970.
- Vaughan, D. G., Comiso, J. C., Allison, I., Carrasco, J., Kaser, G., Kwok, R., Mote, P., Murray, T., Paul, F., Ren, J., Rignot, E., Solomina, O., Steffen, K., and Zhang, T.: Observations: Cryosphere, in: *Climate Change 2013: The Physical Science Basis*, Contribution of Working Group I to the Fifth Assessment Report of the Intergovernmental Panel on Climate Change, edited by: Stocker, T. F., Qin, D., Plattner, G.-K., Tignor, M., Allen, S. K., Boschung, J., Nauels, A., Xia, Y., Bex, V., and Midgley, P. M., Cambridge University Press, Cambridge, United Kingdom and New York, NY, USA, 2013.
- WGMS and NSIDC: World Glacier Inventory, Compiled and made available by the World Glacier Monitoring Service, Zurich, Switzerland, and the National Snow and Ice Data Center, Boulder CO, USA, doi:10.7265/N5/NSIDC-WGI-2012-02, 1989, updated 2012.
- Zemp, M., Haeberli, W., Hoelzle, M., and Paul, F.: Alpine glaciers to disappear within decades?, *Geophys. Res. Lett.*, 33, L13504, doi:10.1029/2006GL026319, 2006.
- Zemp, M., Hoelzle, M., and Haeberli, W.: Distributed modelling of the regional climatic equilibrium line altitude of glaciers in the European Alps, *Global Planet. Change*, 56, 83–100, doi:10.1016/j.gloplacha.2006.07.002, 2007.
- Zwally, H. J., Giovinetto, M. B., Beckley, M. A., and Saba, J. L.: Antarctic and Greenland Drainage Systems, available at: http://icesat4.gsfc.nasa.gov/cryo_data/ant_grn_drainage_systems.php, last access: 7 January 2016, 2012.